



HAL
open science

Adsorption-Induced Deformation in Nanopores: Unexpected Results Obtained by Molecular Simulations

J. Puibasset

► **To cite this version:**

J. Puibasset. Adsorption-Induced Deformation in Nanopores: Unexpected Results Obtained by Molecular Simulations. Sixth Biot Conference on Poromechanics, Jul 2017, Paris, France. pp.547-554, 10.1061/9780784480779.067 . hal-02382471

HAL Id: hal-02382471

<https://hal.science/hal-02382471>

Submitted on 27 Nov 2019

HAL is a multi-disciplinary open access archive for the deposit and dissemination of scientific research documents, whether they are published or not. The documents may come from teaching and research institutions in France or abroad, or from public or private research centers.

L'archive ouverte pluridisciplinaire **HAL**, est destinée au dépôt et à la diffusion de documents scientifiques de niveau recherche, publiés ou non, émanant des établissements d'enseignement et de recherche français ou étrangers, des laboratoires publics ou privés.

Adsorption-Induced Deformation in Nanopores: Unexpected Results Obtained by Molecular Simulations

J. Puibasset, Ph.D.,¹

¹Interfaces, Confinement, Matériaux et Nanostructures, UMR-7374, CNRS, Université d'Orléans, 1b rue de la Férollerie, 45071 Orléans cedex 2, France; e-mail: puibasset@cnrs-orleans.fr

ABSTRACT

The adsorption of a fluid in a nanoporous material induces deformations of the solid. The saturating regime, where the solid is filled with liquid, generally exhibits a linear relationship between the liquid pressure and the solid strain. This provides an experimental way to measure the elastic moduli of the solid walls. For large pores, the strain is determined by the pressure of the liquid saturating the pores and the mechanical properties of the porous solid. What happens at the nanometric scale, where liquid/matrix interfacial effects dominate? We have performed molecular simulations of a simple Lennard-Jones fluid confined between deformable nanoplatelets. The simulations provide the deformation of the nanopore as a function of the liquid pressure, in a way similar to what is done experimentally. The results show unexpected interface effects, which could be relevant to experimental data analysis.

INTRODUCTION

Adsorption-induced deformation of a nanoporous material concerns not only soft materials like biopolymers or aerogels (Dušek 1993; Scherer, Smith *et al.* 1995; Scherer, Smith *et al.* 1995; Thibault, Préjean *et al.* 1995; Herman, Day *et al.* 2006; Kulasinski, Guyer *et al.* 2015; Ogieglo, Wormeester *et al.* 2015), but also stiff materials (Meehan 1927; Bangham and Fakhoury 1928; Haines and McIntosh 1947; Amberg and McIntosh 1952; Scherer 1986; Dolino, Bellet *et al.* 1996; Fomkin 2005; Grosman and Ortega 2009; Prass, Müter *et al.* 2009; Grosman and Ortega 2010; Gor, Paris *et al.* 2013; Schappert and Pelster 2014; Balzer, Braxmeier *et al.* 2015; Grosman, Puibasset *et al.* 2015). Beyond its importance for sequestration, storage or oil recovery (Vandamme, Brochard *et al.* 2010; Brochard, Vandamme *et al.* 2012), it is a fundamental issue to understand the interplay between surface effects and the adsorbed fluid; it has been suggested that deformation could contribute to the hysteresis in the adsorption-desorption isotherm (Haines and McIntosh 1947; Amberg and McIntosh 1952; Grosman and Ortega 2008; Grosman and Ortega 2009; Grosman and Ortega 2010). It is also a powerful tool to measure the elastic moduli

of nanoporous systems (Dolino, Bellet *et al.* 1996; Herman, Day *et al.* 2006; Prass, Mütter *et al.* 2009; Grosman, Puibasset *et al.* 2015).

Understanding the mechanical behavior of nanosized materials has attracted intense searches due to their potential applications. In the case of nanoporous materials, it is possible to use the capillary stress caused by an adsorbed fluid to induce a measurable deformation. A model has to be used to extract the pore moduli from experiments. Poromechanics is a consistent theory to model the mechanical coupling between fluids and solids, including adsorption-induced deformations (Biot 1941; Coussy 2004; Brochard, Vandamme *et al.* 2012; Coasne, Weigel *et al.* 2014; Kulasinski, Guyer *et al.* 2015), but more sophisticated models are required to take into account the inhomogeneous and anisotropic nature of the material (Eriksson 1969; Ash, Everett *et al.* 1973; Ravikovitch and Neimark 2006; Günther and Schoen 2009; Gor and Neimark 2010; Schappert and Pelster 2014; Diao, Fan *et al.* 2016; Gor and Bernstein 2016). It is well-known that porous materials have smaller elastic moduli than the bulk (Gibson and Ashby 1997), but there is generally a disagreement between the measured pore-load moduli and that expected for the porous solid, despite the development of refined models taking into account the pore geometry (Gor, Bertinetti *et al.* 2015; Guyer and Kim 2015; Liu, Wu *et al.* 2016; Rolley, Garroum *et al.* 2017).

The surface stress is dominant in nanometer size systems, and generally taken into account in the models to calculate the elastic constants of the solid. However, the interplay between surface stress and adsorption is not so well documented. We thus perform a “numerical experiment” of adsorption-induced deformation of a nanoplatelet. The advantages are the following: the geometry is perfectly known, and the elastic constants of the solid, taking into account the surface stress, is known too. The observed deformation can thus be compared to that expected from the porous solid modulus and a theoretical thermodynamic approach. The observed discrepancy suggests an influence of the adsorbed fluid on the surface stress of the solid.

The atomistic model and the thermodynamic approach are presented in the next section. In the third section we present the results and question the validity of the macroscopic approach.

MODEL AND NUMERICAL DETAILS

Solid. The platelet is chosen to be a fcc Lennard-Jones (12,6) solid, with parameters $\varepsilon=73.2$ kJ/mol and $\sigma=0.3518$ nm. The interactions are cut at 4σ . These values allow reproducing the mechanical properties of silicon, a material that has been used several times to study adsorption-induced deformation (Dolino, Bellet *et al.* 1996; Grosman, Puibasset *et al.* 2015). Note however that silicon is not a fcc solid, and that better potentials exist to reproduce its physical properties (Lee 2007). The fcc Lennard-Jones solid is however accurate enough for our purpose. The bulk properties are determined in a simulation box containing 6 unit cells (3.26 nm) in each direction with periodic boundary conditions (the crystallographic axes are parallel to the simulation box). The Young modulus E and the Poisson coefficient ν have been determined by Monte Carlo simulations in the isobaric ensemble where an external pressure is applied on the

system and the average deformation is an output of the simulation. We obtain $E = 165$ GPa and $\nu = 0.36$ at 300 K. The shear modulus is not used in this work. Note that the symmetry of the solid being cubic, the mechanical properties are entirely given by E and ν .

The properties of the nanoplatelet are evaluated in a larger simulation box: $L_x = L_y = 7$ unit cells in the x and y directions (3.805 nm); a gap is introduced along the z direction so as to create two opposite surfaces (see Fig. 1, left). The thickness h of the nanoplatelet is 6 unit cells ($h = 3.26$ nm), and the dimension $L_z = 10$ nm. The distance between the walls is thus $H = 6.74$ nm. The wall thickness is quite small (compared to typical nanoporous silicon for instance, 5-6 nm), in order to emphasize surface stress effects. The gap is however typical of nanoporous materials. The elastic properties of the platelet have been determined in the framework of the standard Monte Carlo simulations in the isobaric ensemble, where only the dimensions parallel to the nanoplatelet are allowed to vary, while L_z is fixed. The cubic symmetry of the solid reduces to the tetragonal symmetry for the nanoplatelet, which requires the determination of 4 parameters to get the compliance matrix: $E_x = 162$ GPa, $E_z = 180$ GPa, $\nu_{yx} = 0.457$, $\nu_{zx} = 0.339$, and $\nu_{xz} = 0.335$ at 353 K. Note that these elastic moduli take into account the surface stress.

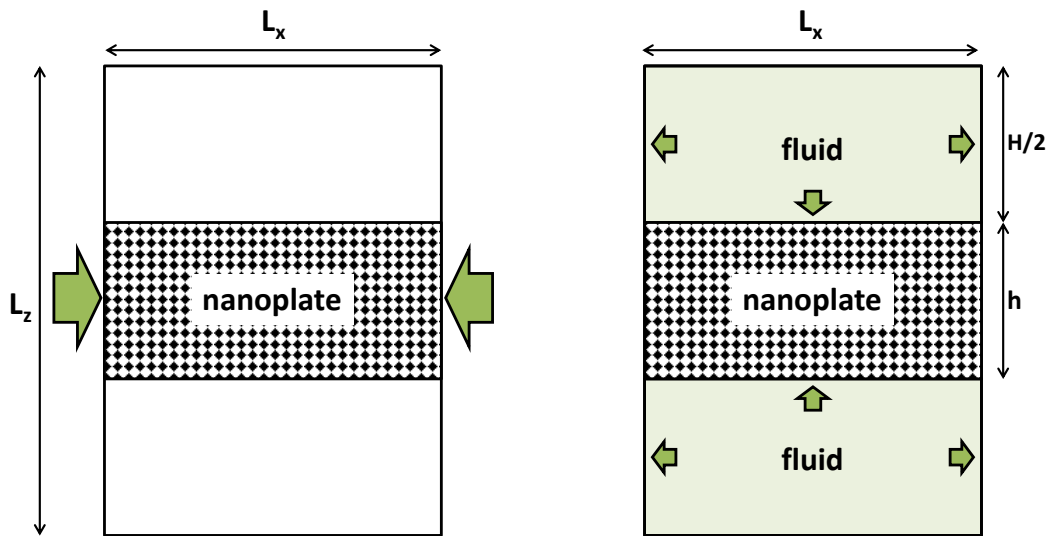


Figure 1. General presentation of the simulation box; L_z is constant, while L_x and L_y are allowed to fluctuate (isobaric ensemble). Left: an external pressure (arrows) is imposed to measure the elastic moduli of the nanoplatelet. Right: a fluid at imposed chemical potential is introduced; the external pressure is set to zero; the arrows materialize the internal pressure of the fluid.

Fluid. Since we focus on non-specific effects between the fluid and the substrate we use again the Lennard-Jones (12,6) potential to model the fluid-fluid and fluid-solid interactions. Following Watanabe *et al.* (Watanabe, Ito *et al.* 2012), the potential is truncated at 3σ and a quadratic term is added so that both the potential and force are continuous. The parameters are chosen to mimic n-heptane, a non-polar fluid which has been used previously for experiments (Grosman,

Puibasset *et al.* 2015). The fluid-fluid parameters are $\sigma_{ff} = 0.6$ nm and $\varepsilon_{ff}/k = 505$ K, where k is Boltzmann's constant, or $\varepsilon_{ff} = 4.2$ kJ/mol, and the fluid-wall parameters are taken equal to the fluid-fluid parameters. Calculations are performed at 353 K, just above the freezing point of the Lennard-Jones model. Using standard grand canonical Monte Carlo simulations, the pressure of the (bulk) liquid phase has been determined versus its chemical potential μ (see Table 1). Note that we have considered μ values above and below (metastable liquid) its bulk saturating value, because, in the system we want to study, the fluid is confined (Puibasset 2005). The pressure of the liquid phase thus ranges from -116 to +210 bar.

Method. The method relies on the measurement of the deformation of the solid induced by the pressure of the adsorbed fluid (see Fig. 1, right). We use the standard semi-grand canonical Monte Carlo algorithm to let the simulation box fluctuate in the x and y directions while the chemical potential of the fluid is imposed through the pressure of the surrounding gas. The external pressure on the simulation box is set to zero: the system is free to relax, so that the solid (which deforms) accommodates the fluid pressure.

Phenomenological model. The aim of this section is to relate the expected average deformation of the simulation box with the fluid pressure, in the framework of a simple thermodynamic approach. The quantities to be considered are: the pressure of the liquid adsorbed on the platelet, P_L ; the fluid-wall surface tension γ , and the elastic moduli of the platelet previously determined without adsorbed fluid. At equilibrium, the overall constrain on the simulation box walls parallel to the z axis is zero since the external pressure in the semi-grand canonical ensemble is set to zero (free walls). As a consequence

$$\sigma_{xx} = \sigma_{yy} = (H P_L - \gamma L_x L_y)/h; \quad \sigma_{zz} = -P_L$$

where γ is the solid-fluid surface tension. Deformations along the x and y directions are given by:

$$\begin{aligned} \varepsilon_{xx} = \varepsilon_{yy} &= (1-\nu_{yx}) \sigma_{xx}/E_x - \nu_{zx}\sigma_{zz}/E_z \\ &= [(1-\nu_{yx})H/(E_x h) + \nu_{zx}/E_z] P_L - \gamma (1-\nu_{yx}) L_x L_y / (E_x h). \end{aligned}$$

The surface tension, given by the excess amount of adsorbed liquid, is essentially constant because the liquid is barely compressible. The solid deformation is thus expected to be linear with the liquid pressure; the inverse of the slope is $[(1-\nu_{yx})H/(E_x h) + \nu_{zx}/E_z]^{-1} = 113$ GPa. Note that the fluid pressure has two additive effects on the solid: through the simulation box (a positive pressure tends to dilate the nanoplatelet in the x and y directions), and directly on the solid (a positive fluid pressure along z induces a nanoplatelet dilatation along x and y given by the Poisson ratio).

TABLE 1: Monte Carlo simulation results.

ln(activity)	-11.175	-10.83	-10.485	-10.200	-9.930	-9.375
P_L (bar)	-119	-65	-1.9	52.1	113	211
$\varepsilon_{xx} = \varepsilon_{yy}$	-5.65×10^{-5}	-1.85×10^{-5}	8.86×10^{-6}	2.80×10^{-5}	4.99×10^{-5}	8.91×10^{-5}

RESULTS AND DISCUSSION

For each given chemical potential, we have measured the fluctuations of the system size in directions x and y (see an example in Fig. 2). The fluctuations are of the order of $10^{-3} L_x$, which means that they are not negligible compared to the average deformation of the nanoplatelet, as expected in nanometer size systems. Long simulation runs are thus required to reach an accuracy of 5% in the determination of the solid strain.

The average strain has been determined for different values of the chemical potential. The results are given in Table 1. As can be seen, the solid deforms under the influence of the adsorbed fluid. For high chemical potential values, the solid expands, while for low chemical potential values the solid shrinks. This is qualitatively expected from the observation that the fluid pressure acts directly on the solid (along z) and through the simulation box (parallel to the nanoplatelet). The observed deformation is of order 10^{-4} , typical of solid strain.

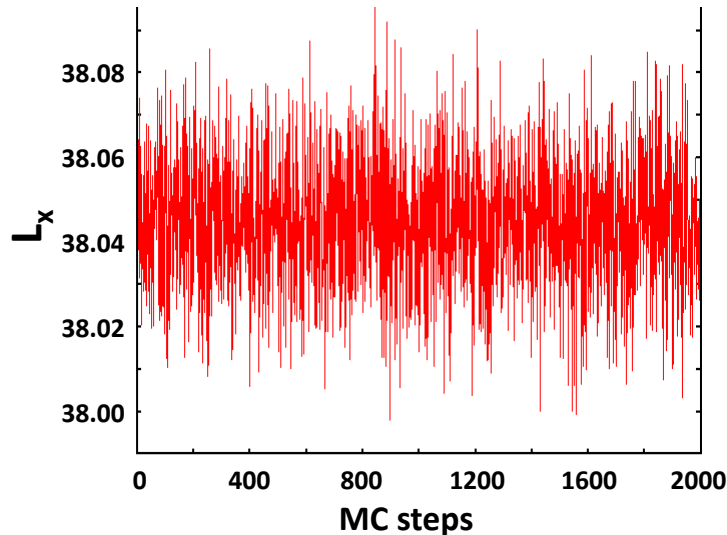


Figure 2. Fluctuations of the nanoplatelet dimension L_x during a Monte Carlo simulation run. 1 MC step corresponds to 1000 moves per atom.

The simulation results are shown as a function of the liquid pressure in Fig. 3. As can be seen, the observed strain follows essentially a linear behavior, except for the lowest pressure point, which however corresponds to the stability limit of the stretched liquid. At coexistence, where the liquid pressure is essentially zero, the observed deformation is very small: the solid-fluid surface tension is thus small compared to the solid stiffness. How do the simulations compare with the phenomenological model depicted in previous section? The prediction of the model is given as a solid line in Fig. 3, where we have omitted the (constant) surface tension term. The simulations qualitatively follow the expected behavior (linear), but a significant disagreement is observed between the slopes. The inverse of the slope of the simulation results is approximately 270 GPa, while the prediction gives 113 GPa.

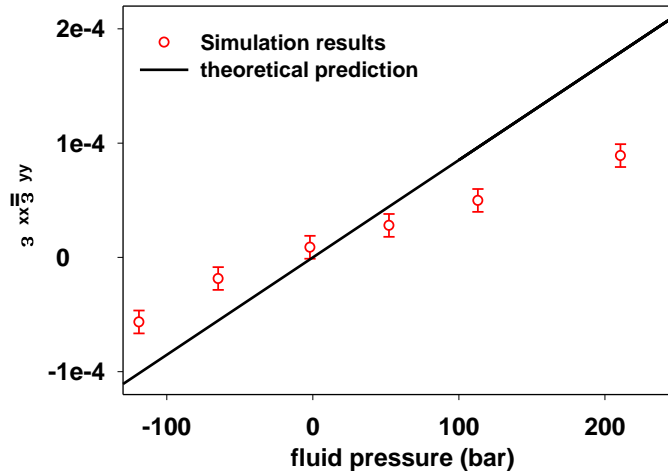


Figure 3. Symbols: Monte Carlo simulation results of the nanoplalelet deformation as a function of the fluid pressure in the liquid phase (the line is a guide to the eye). Solid black line: theoretical prediction based on the thermodynamic approach (see text).

Many papers in the literature mention disagreements between the elastic moduli determined from adsorption-induced deformation measurements and bulk values. Two major origins are invoked. On one hand, the origin is attributed to finite size effects due to the small wall thicknesses in nanoporous materials. On the other hand, one can also invoke the dependence of the solid (surface) stress with the presence of the adsorbed fluid.

Since in our simulations the elastic constants have been determined for the nanoplalelet itself, finite size and surface stress effects cannot be invoked to explain the disagreement. Two hypotheses are proposed to explain the results: a strong dependence of the fluid-substrate free energy with the chemical potential of the fluid, or a significant variation of the surface stress of the solid in presence of the fluid. The small compressibility of the adsorbed liquid seriously disfavors the first hypothesis. However, quantitative analysis is under consideration. The second argument has already been invoked to explain some features of the nitrogen adsorption hysteresis in porous silicon (Grosman and Ortega 2008; Grosman and Ortega 2009; Grosman and Ortega 2010).

CONCLUSION

This paper focused on the comparison between the adsorption-induced deformation of a nanoplalelet given by atomistic simulations, and that predicted from the elastic constants of the nanoplalelet determined without fluid. The results show a strong disagreement which could reveal interplay between surface stress and fluid adsorption.

ACKNOWLEDGMENTS

The author acknowledges fruitful discussions with A. Grosman and E. Rolley on experimental and theoretical issues regarding adsorption-induced deformation.

REFERENCES

- Amberg, C. H. and McIntosh, R. (1952). "A Study of Adsorption Hysteresis by Means of Length Changes of a Rod of Porous Glass." *Can. J. Chem.* 30(12): 1012-1032.
- Ash, S. G., Everett, D. H., *et al.* (1973). "Thermodynamics of the Effects of Adsorption on Interparticle Forces." *J. Chem. Soc., Faraday Trans. 2* 69(0): 1256-1277.
- Balzer, C., Braxmeier, S., *et al.* (2015). "Deformation of Microporous Carbon During Adsorption of Nitrogen, Argon, Carbon Dioxide, and Water Studied by in Situ Dilatometry." *Langmuir* 31(45): 12512-12519.
- Bangham, D. H. and Fakhoury, N. (1928). "The Expansion of Charcoal Accompanying Sorption of Gases and Vapours." *Nature* 122: 681-682.
- Biot, M. A. (1941). "General Theory of Three-Dimensional Consolidation." *J. Appl. Phys.* 12(2): 155-164.
- Brochard, L., Vandamme, M., *et al.* (2012). "Poromechanics of Microporous Media." *J. Mech. Phys. Solids* 60(4): 606-622.
- Coasne, B., Weigel, C., *et al.* (2014). "Poroelastic Theory Applied to the Adsorption-Induced Deformation of Vitreous Silica." *J. Phys. Chem. B* 118(49): 14519-14525.
- Coussy, O. (2004). *Poromechanics*. New York, John Wiley & Sons.
- Diao, R., Fan, C., *et al.* (2016). "Monte Carlo Simulation of Adsorption-Induced Deformation in Finite Graphitic Slit Pores." *J. Phys. Chem. C* ASAP.
- Dolino, G., Bellet, D., *et al.* (1996). "Adsorption Strains in Porous Silicon." *Phys. Rev. B* 54(24): 17919-17929.
- Dušek, K. (1993). "Responsive Gels: Volume Transitions I." *Adv. Polym. Sci.* 109.
- Eriksson, J. C. (1969). "Thermodynamics of Surface Phase Systems." *Surf. Sci.* 14(1): 221-246.
- Fomkin, A. A. (2005). "Adsorption of Gases, Vapors and Liquids by Microporous Adsorbents." *Adsorption* 11(3): 425-436.
- Gibson, L. J. and Ashby, M. F. (1997). *Cellular Solids: Structure and Properties*. Cambridge, Cambridge University Press.
- Gor, G. Y. and Bernstein, N. (2016). "Revisiting Bangham's Law of Adsorption-Induced Deformation: Changes of Surface Energy and Surface Stress." *Phys. Chem. Chem. Phys.* 18(14): 9788-9798.
- Gor, G. Y., Bertinetti, L., *et al.* (2015). "Elastic Response of Mesoporous Silicon to Capillary Pressures in the Pores." *Appl. Phys. Lett.* 106(26): 261901.
- Gor, G. Y. and Neimark, A. V. (2010). "Adsorption-Induced Deformation of Mesoporous Solids." *Langmuir* 26(16): 13021-13027.
- Gor, G. Y., Paris, O., *et al.* (2013). "Adsorption of N-Pentane on Mesoporous Silica and Adsorbent Deformation." *Langmuir* 29: 8601-8608.
- Grosman, A. and Ortega, C. (2008). "Influence of Elastic Deformation of Porous Materials in Adsorption-Desorption Process: A Thermodynamic Approach." *Phys. Rev. B* 78: 085433.
- Grosman, A. and Ortega, C. (2009). "Influence of Elastic Strains on the Adsorption Process in Porous Materials: An Experimental Approach." *Langmuir* 25(14): 8083-8093.
- Grosman, A. and Ortega, C. (2010). "Influence of Elastic Strains on the Adsorption Process in Porous Materials. Thermodynamics and Experiments." *Appl. Surf. Sci.* 256(17): 5210-5215.
- Grosman, A., Puibasset, J., *et al.* (2015). "Adsorption-Induced Strain of a Nanoscale Silicon Honeycomb." *Europhys. Lett.* 109(5): 56002.

- Günther, G. and Schoen, M. (2009). "Sorption Strains and Their Consequences for Capillary Condensation in Nanoconfinement." *Mol. Simul.* 35(1-2): 138-150.
- Guyer, R. A. and Kim, H. A. (2015). "Theoretical Model for Fluid-Solid Coupling in Porous Materials." *Phys. Rev. E* 91(4): 042406.
- Haines, R. S. and McIntosh, R. (1947). "Length Changes of Activated Carbon Rods Caused by Adsorption of Vapors." *J. Chem. Phys.* 15(1): 28-38.
- Herman, T., Day, J., *et al.* (2006). "Deformation of Silica Aerogel During Fluid Adsorption." *Phys. Rev. B* 73(9): 094127.
- Kulasinski, K., Guyer, R., *et al.* (2015). "Poroelastic Model for Adsorption-Induced Deformation of Biopolymers Obtained from Molecular Simulations." *Phys. Rev. E* 92(2): 022605.
- Lee, B.-J. (2007). "A Modified Embedded Atom Method Interatomic Potential for Silicon." *Calphad* 31(1): 95-104.
- Liu, M., Wu, J., *et al.* (2016). "The Pore-Load Modulus of Ordered Nanoporous Materials with Surface Effects." *AIP Advancies* 6(3): 035324.
- Meehan, F. T. (1927). "The Expansion of Charcoal on Sorption of Carbon Dioxide." *Proc. R. Soc. London A* 115(770): 199-207.
- Ogieglo, W., Wormeester, H., *et al.* (2015). "In Situ Ellipsometry Studies on Swelling of Thin Polymer Films: A Review." *Prog. Polym. Sci.* 42: 42-78.
- Prass, J., Mütter, D., *et al.* (2009). "Capillarity-Driven Deformation of Ordered Nanoporous Silica." *Appl. Phys. Lett.* 95(8): 083121.
- Puibasset, J. (2005). "Grand Potential, Helmholtz Free Energy, and Entropy Calculation in Heterogeneous Cylindrical Pores by the Grand Canonical Monte Carlo Simulation Method." *J. Phys. Chem. B* 109(1): 480-487.
- Puibasset, J. (2005). "Thermodynamic Characterization of Fluids Confined in Heterogeneous Pores by Monte Carlo Simulations in the Grand Canonical and the Isobaric-Isothermal Ensembles." *J. Phys. Chem. B* 109(16): 8185-8194.
- Ravikovitch, P. I. and Neimark, A. V. (2006). "Density Functional Theory Model of Adsorption Deformation." *Langmuir* 22(26): 10864-10868.
- Rolley, E., Garroum, N., *et al.* (2017). "Using capillary forces to determine the elastic properties of mesoporous materials." *Phys. Rev. B* 95, 064106 (2017).
- Schappert, K. and Pelster, R. (2014). "Unexpected Sorption-Induced Deformation of Nanoporous Glass: Evidence for Spatial Rearrangement of Adsorbed Argon." *Langmuir* 30(46): 14004-14013.
- Scherer, G. W. (1986). "Dilatation of Porous Glass." *J. Am. Ceram. Soc.* 69(6): 473-480.
- Scherer, G. W., Smith, D. M., *et al.* (1995). "Compression of Aerogels." *J. Non-Cryst Solids* 186: 316-320.
- Scherer, G. W., Smith, D. M., *et al.* (1995). "Deformation of Aerogels During Characterization." *J. Non-Cryst Solids* 186: 309-315.
- Thibault, P., Préjean, J. J., *et al.* (1995). "Silica-Aerogel Thermal Expansion Induced by Submonolayer Helium Adsorption." *Phys. Rev. B* 52(24): 17491-17500.
- Vandamme, M., Brochard, L., *et al.* (2010). "Adsorption and Strain: The CO₂-Induced Swelling of Coal." *J. Mech. Phys. Solids* 58(10): 1489-1505.
- Watanabe, H., Ito, N., *et al.* (2012). "Phase Diagram and Universality of the Lennard-Jones Gas-Liquid System." *J. Chem. Phys.* 136(20): 204102.